

# On the Simulation of Single Electron Transport in a Strongly Disordered Medium

Mohammad Javadi and Yaser Abdi\*

*Department of Physics, University of Tehran, Tehran 14395-547, Iran*

(Dated: January 27, 2023)

Mesoscopic modeling of electron transport in disordered organic and inorganic materials is based on the many-particle Monte-Carlo simulation. The main disadvantage of this method is that the simulation becomes significantly slower by increasing electron concentration. This problem makes it almost impossible to gain information about electron transport at higher Fermi levels. Recently a single-particle Monte-Carlo method based on the modified (truncated) density of localized states has been proposed which benefits from very short time execution. Although the truncated single-particle method can successfully clarifies the properties of electron transport in moderately disordered systems, utilizing this method for a strongly disordered medium may be accompanied by severe shortcomings which are mainly originated from zero temperature approximation and spatial occupation of localized states. Depending on the characteristic energy of localized states, Fermi level and the temperature of system, deviation the results of truncated model from theoretical predictions can be very large (orders of magnitude). Here, a single-particle method based on the modified residence time of electron in the localized states is proposed which successfully reproduce the theoretical predictions in the strongly disordered systems. The proposed model is justified by comparing the analytical calculations and computer simulations for a wide range values of disorder parameter, Fermi level and temperature.

PACS numbers: 61.43.Bn, 72.20.Ee, 72.80.Ng, 66.30.Pa

Inorganic nano-crystalline and micro-crystalline metal oxide materials such as titania and zinc oxide have been drawing a lot of attention due to their photovoltaic and photocatalytic applications.<sup>1–3</sup> In the most of these applications electron transport plays a key role in the overall performance of the device. Therefore description and modeling the electron transport is very important for optimization of the device performance. Because of structural disorder, the electronic states in the these materials are localized and the density of localized states (DOLS) is given by<sup>4,5</sup>

$$g(E) = \alpha \frac{N_t}{KT} \exp(\alpha \frac{E}{KT}) \quad (1)$$

where  $\alpha$  is energy disorder parameter and is related to the characteristic temperature of localized states as  $\alpha = T/T_0$ .<sup>6</sup>  $N_t$  is total density of localized states and  $E$  is energy of states with respect to a reference level (conduction band edge  $E_0$  or transport level  $E_l$ ).<sup>7,8</sup> Mesoscopic description of the electron transport in such disordered media is based on the Monte-Carlo random walk simulation which offers exhaustive approaches for investigation of different morphological and energetic aspects of electrons transport.<sup>9–13</sup> In all cases the effect of Fermi level on the electron transport constructs the most important part of these studies. For this end, two alternative approaches based on the many-particle simulation have been developed. In the first approach the Fermi level is considered as an input parameter of the simulation<sup>13,14</sup> and in the second one the Fermi level is counted as a well-defined output parameter which is calculated from the ratio of visited states and  $g(E)$ .<sup>15,16</sup> The common disadvantage of both models is the amount of time taken for simulation implementation. Depending on the values of parameters, up to one hundred hours may be spent for

a single implementation which is obviously undesirable. However, quite generally, once the density of electrons is less than the total density of localized states (i.e. the electron-electron interactions can be ignored), the single-particle simulation with the benefit of short time implementation can be used. The single-particle simulation is based on the modified DOLS which is given by<sup>16</sup>

$$g(E) = H(E - E_f) \alpha \frac{N_t}{KT} \exp(\alpha \frac{E}{KT}) \quad (2)$$

where  $H$  is Heaviside step function (Fig. 1). This modification is based on the fact that for a reasonable period of time (i.e. not very long times), the transport properties of the system are governed solely by the electrons with energies around  $E_f$ .<sup>14</sup> It was shown that the single-particle simulation can approximately reproduce many-particle results<sup>16</sup> leading to a growing trend in the use of single-particle procedure.<sup>17–24</sup> Nonetheless, utilizing this method for a strongly disordered medium may be accompanied by severe shortcomings. Such limitations originate predominantly from zero temperature approximation in the truncated DOLS (Eq. 2) and the spatial occupation of localized states which is ignored in the truncated model. Eq. 2 is based on the zero temperature approximation where the Fermi-Dirac distribution ( $f_{FD}(E)$ ) is replaced by a step function. However, in the framework of both multiple trapping regime and hopping regime, the transport mechanism is thermally activated (i.e. the conductance vanishes as  $T \rightarrow 0$ ). In addition, it is implicitly assumed that the average distance between unoccupied states remains constant. This assumption looks to be incorrect as the Fermi level increases. The

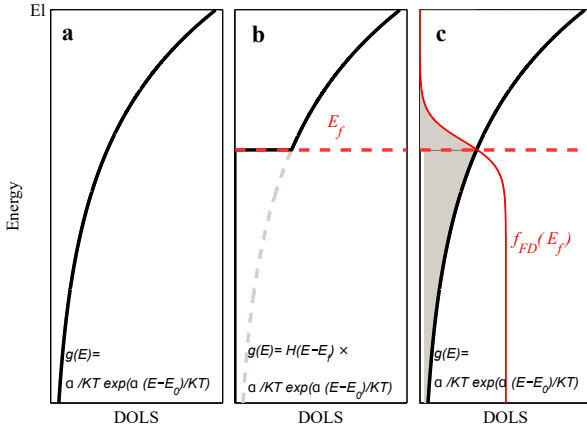


FIG. 1. (a) Exponential density of localized states. (b) Truncated density of localized states used in the conventional single-particle simulations (model 1). (c) Schematic of modified simulation of single-particle transport (model 2). Gray region indicates the occupied states.

density of unoccupied states can be calculated as

$$N_{imp} = \int_{-\infty}^{E_l=0} g(E)(1 - f_{FD}(E))dE \quad (3)$$

$$N_{imp} = \frac{\alpha}{1 + \alpha} N_t e^{-\epsilon_f} {}_2F_1(1, 1 + \alpha, 2 + \alpha, -e^{-\epsilon_f}) \quad (4)$$

where  ${}_2F_1$  is Gauss hypergeometric function and  $\epsilon_f = E_f/KT$ . Assuming a homogenous distribution of localized states, the average distance between unoccupied sites may be obtained as  $a_l = N_{imp}^{-1/3}$ . As it can be seen from Fig. 2 by decreasing  $\alpha$  (being more disorder) the average distance between unoccupied sites increases. Comparing with the analytical calculations, we will show that these drawbacks may guide to considerably deviations in the estimation of transport coefficients. Our aim is to propose an alternative approach based on the modification of transport mechanism which is able to successfully reproduce the theoretical predictions while it benefits from fast implementation.

The simulations were carried out in a  $50 \times 50 \times 50$  simple cubic lattice with a lattice constant of  $a_0$ . In the conventional continuous-time random walk single-particle simulations (here after will be referred as *model 1*), at a desired Fermi level the energies of localized states are calculated according to the Eq. 2. For thermally-activated transport and in the framework of semi-classical multiple trapping, the electron residence time in each trap site is given by<sup>25,26</sup>

$$t_i = \ln(R)\nu_0^{-1} \exp\left(\frac{E_i - E_l}{KT}\right) \quad (5)$$

here  $\nu_0$  is thermal frequency ( $\sim$ THz)<sup>27</sup> and  $R$  is a random number uniformly distributed between 0 and 1. The simulation begins with placing an electron randomly at

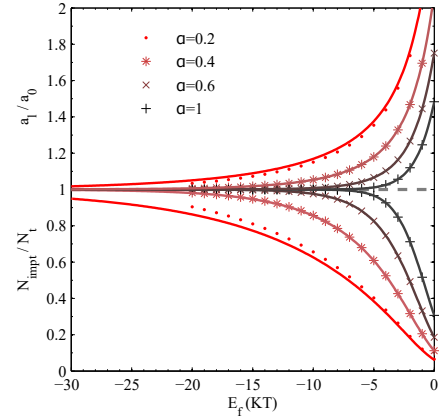


FIG. 2. The fraction of unoccupied states and the average distance between unoccupied sites as a function of Fermi level. Marks and lines represent the results of Monte-Carlo simulation and Eq. 4 respectively.

one of the sites. Then the transport time is advanced by residence time of that site and the electron is allowed to move randomly into one the nearest neighbors. In thermal equilibrium the electron diffusion exhibits non-dispersive character (i.e. at sufficiently long times)<sup>14,28,29</sup> and the jump (tracer) diffusion coefficient can be calculated by<sup>16,30</sup>

$$D_J = \frac{\langle r^2(t) \rangle}{6t} \quad (6)$$

where  $\langle r^2(t) \rangle$  is mean-squared displacement and  $t$  is total transport time. The outlines of modified single-particle simulation (here after will be referred as *model 2*) is as follows. The energies of trap sites are computed according to the raw DOLS Eq. 1 while the electron residence time is modified as

$$t_i = (1 - F_i) \ln(R) \nu_0^{-1} \exp\left(\frac{E_i - E_l}{KT}\right) + \tau \quad (7)$$

In this equation  $\tau$  is relaxation time constant for elastic scatterings in delocalized states and  $F_i$  indicates the probability of occupation of the site which is calculated with respect to Fermi-Dirac distribution

$$F_i = \begin{cases} 0 & \text{if } Rnd(0,1) > f_{FD}(E_i - E_f) \\ 1 & \text{if } Rnd(0,1) \leq f_{FD}(E_i - E_f) \end{cases}$$

Accordingly in the model 2, the trapping/detrapping events are taken into account only for unoccupied states (Fig. 1). By this modification, beside of keeping the advantage of fast implementation, temperature effects as well as spatial occupation effects are considered simultaneously in the simulation process. In order to reduce statistical fluctuations, in all of the simulations the electron transport coefficient was obtained by averaging over 200 runs.

Fig. 3 represents temporal evaluation of electron diffusion coefficient for  $\alpha = 0.2$  and  $\alpha = 0.6$ . It is seen that in

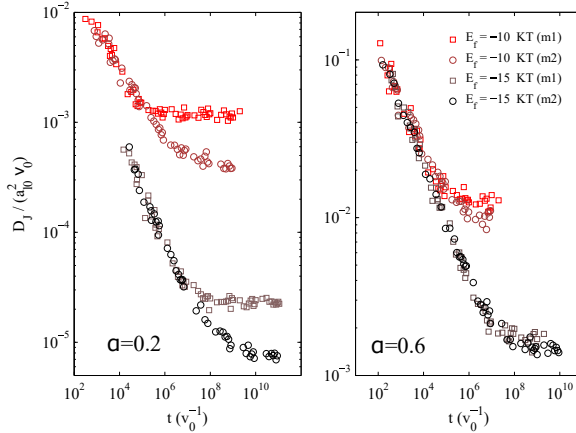


FIG. 3. Temporal evaluation of normalized electron diffusion coefficient obtained from simulations based on model 1 (indicated by m1) and model 2 (indicated by m2) for  $T = 300K$  and  $z = \nu_0\tau = 10^{-4}$ . The non-dispersive transport is defined as a region for which  $dD_J/dt = 0$ .

the region of dispersive transport the slope of two models are identical. However, according to the results of model 2, at  $\alpha = 0.2$  the normal diffusion process begins at longer times compared with model 1 (about two orders of magnitude). As  $\alpha$  increases (being less disordered) the difference between two models vanishes. This observation is a direct consequence of spatial occupation of sites. In all steps in model 1, the electron encounters with an unoccupied site. Consequently, the sampling rate from localized states is high and the thermal equilibrium with localized states is obtained at shorter times. On the other hand, in the framework of model 2 a visited trap site can be either occupied or unoccupied leading to a sampling rate typically smaller than model 1. So it is expected that in model 2 the thermal equilibrium is obtained at longer times. Since at a fixed Fermi level, the fraction of occupied states decreases by increasing  $\alpha$  (Fig. 2), the equilibrium is obtained almost at the same time for two models.

Theoretically the static electron diffusion coefficient is given by<sup>16</sup>

$$D_J = \frac{1}{6} \left(1 - \frac{T}{T_0}\right) \exp\left(\frac{E_f - E_l}{KT} \left(1 - \frac{T}{T_0}\right)\right) \quad (8)$$

Fig. 4 shows the simulation results of electron diffusion coefficient vs. Fermi level carried out at different values of  $\alpha$ . It is seen that at  $\alpha = 0.6$ , the results obtained from two models are identical and consistent with Eq. 8. In contrast, as the value of  $\alpha$  decreases (being more disorder) the results of model 1 deviate from theoretical predictions and this deviation grows exponentially by reducing Fermi level. Similar deviations have been reported by other groups.<sup>16,17</sup> On the other hand, as it can be confirmed from Fig. 4, the results of modified model (model 2) are quite consistent with the analytical Eq. 8 for total range of  $\alpha$  and  $E_f$ .

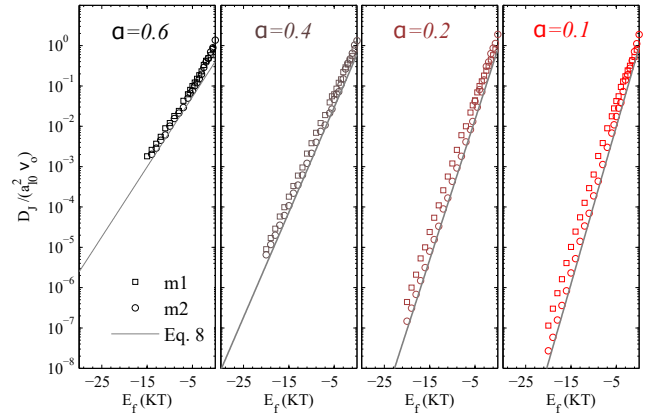


FIG. 4. Electron diffusion coefficient vs. Fermi level at  $T = 300K$  and  $z = \nu_0\tau = 10^{-4}$ . Squares, circles and lines indicate respectively the results of model 1, model 2 and the theoretical Eq. 8

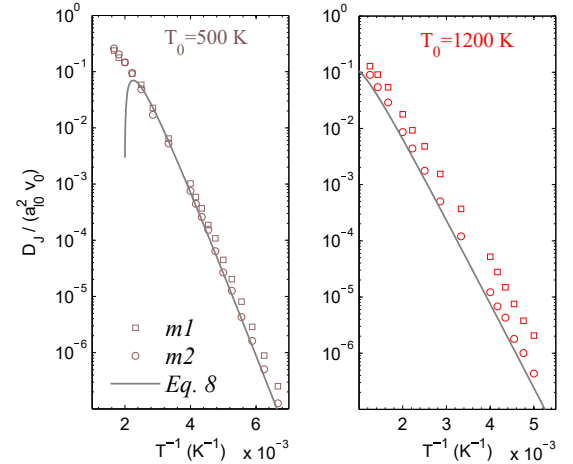


FIG. 5. Electron diffusion coefficient vs. temperature at constant Fermi level -0.3 eV.

Variation of electron diffusion coefficient with respect to inverse temperature is shown in Fig. 5. In both models, simulations were carried out at a constant Fermi level of -0.3 eV. Again, it is seen that as disorder (characteristic temperature of localized states,  $T_0$ ) increases, the results of model 1 become inconsistent with the theoretical line while for different values of  $T_0$  and total range of  $T^{-1}$  the results of proposed model retain their consistency with the Eq. 8. It is worth noting that due to the exponential dependence of residence time on the temperature (Eq. 5 and Eq. 7), two models converge as temperature increases.

The results presented in Fig. 3 – Fig. 5 are based on the nearest neighbor movement for which  $r_{cut} = a_0$ . Since multiple trapping model does not depend on the distance between localized states, the zone of possible target sites can be enlarged arbitrary in order to reproduce practically observations. In order to investigate the

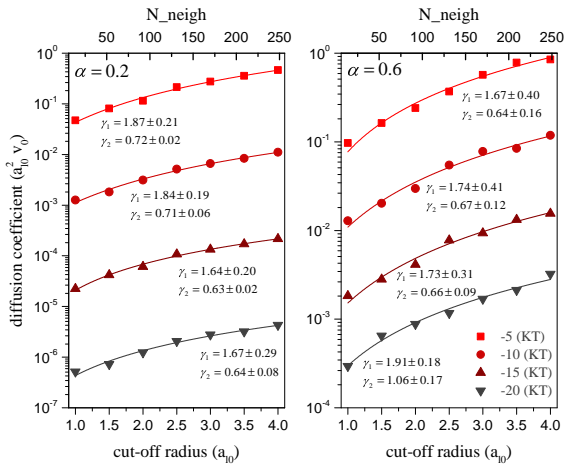


FIG. 6. Diffusion coefficient as a function of cut-off radius (total number of accessible sites) at different Fermi levels. The values of  $\gamma_1$  and  $\gamma_2$  obtained by nonlinear curve fitting tools of ORIGIN.

effect of cut-off radius on the electron diffusion coefficient, the simulations were repeated for different values of cut-off radius and the results are summarized in Fig. 6. Assuming a power law relation  $D_J \propto r_{cut}^{\gamma_1}$ , it is observed that for a simple cubic lattice both models conduct to almost the same result of  $\gamma_1 = 1.6 - 1.9$  (Fig. 6). This result appears to be inconsistent with  $D_J \propto r_{cut}^3$

discussed elsewhere.<sup>31</sup> The upper *x* axis in the plots of Fig. 6 denotes the total number of neighbors. Utilizing a power law relation of  $D_J \propto N_{neigh}^{\gamma_2}$  it was found that  $\gamma_2 = 0.6 - 0.7$ . Since the total number of neighbors increases as  $N_{neigh} \propto r_{cut}^3$  it is expected that  $\gamma_2 = \gamma_1/3$  which is observed in Fig. 6.

In conclusion, it was shown that in the presence of strong disorder, the procedure of conventional single-particle simulation which is based on the truncated distribution of localized states may considerably deviates from theoretical predictions. The origins of the deviations were discussed on the bases of zero temperature approximation and spatial occupation of localized states. The proposed model which is based on the modified residence time (rather than modified DLOS) can reproduce successfully the analytical results for a wide range of different parameters. It is expected that the proposed model can also be used for hopping regime where the transition rate between two localized states is directly related to the the distance between them as  $p_{i \rightarrow j} = \nu_0^{-1} \exp(-2r/\xi - \epsilon_{ji}/KT)$ .<sup>17,32</sup> Eventually it should be emphasized that the truncated DOLS model is quite applicable for moderate disorders.

The authors wish to thank the Iran National Science Foundation (INSF) for partial financial support. Partial financial support from the Centre of Excellence on the Structure of Matter of the University of Tehran is also acknowledged.

\* y.abdi@ut.ac.ir

- <sup>1</sup> Y. Bai, I. Mora-Sero, F. De Angelis, J. Bisquert, and P. Wang, Chemical reviews **114**, 10095 (2014).
- <sup>2</sup> Y. Jin, J. Wang, B. Sun, J. C. Blakesley, and N. C. Greenham, Nano letters **8**, 1649 (2008).
- <sup>3</sup> M. S. Alvar, M. Javadi, Y. Abdi, and E. Arzi, Journal of Applied Physics **119**, 114302 (2016).
- <sup>4</sup> J. Nelson, S. A. Haque, D. R. Klug, and J. R. Durrant, Physical Review B **63**, 205321 (2001).
- <sup>5</sup> J. Nelson, Physical Review B **59**, 15374 (1999).
- <sup>6</sup> M. Mandoc, B. de Boer, G. Paasch, and P. Blom, Physical Review B **75**, 193202 (2007).
- <sup>7</sup> I. Fishchuk, A. Kadaschchuk, A. Bholokam, A. d. J. de Meux, G. Pourtois, M. Gavrilyuk, A. Köhler, H. Bässler, P. Heremans, and J. Genoe, Physical Review B **93**, 195204 (2016).
- <sup>8</sup> P. T. Erslev, H.-Y. Chen, J. Gao, M. C. Beard, A. J. Frank, J. van de Lagemaat, J. C. Johnson, and J. M. Luther, Physical Review B **86**, 155313 (2012).
- <sup>9</sup> J. Van de Lagemaat, K. D. Benkstein, and A. J. Frank, The Journal of Physical Chemistry B **105**, 12433 (2001).
- <sup>10</sup> K. D. Benkstein, N. Kopidakis, J. Van de Lagemaat, and A. Frank, The Journal of Physical Chemistry B **107**, 7759 (2003).
- <sup>11</sup> A. Barzykin and M. Tachiya, The Journal of Physical Chemistry B **106**, 4356 (2002).
- <sup>12</sup> M. J. Cass, F. Qiu, A. B. Walker, A. Fisher, and L. Peter, The Journal of Physical Chemistry B **107**, 113 (2003).
- <sup>13</sup> J. Nelson and R. E. Chandler, Coordination Chemistry Reviews **248**, 1181 (2004).
- <sup>14</sup> J. Van de Lagemaat and A. Frank, The Journal of Physical Chemistry B **105**, 11194 (2001).
- <sup>15</sup> J. A. Anta, J. Nelson, and N. Quirke, Physical Review B **65**, 125324 (2002).
- <sup>16</sup> J. A. Anta, I. Mora-Seró, T. Dittrich, and J. Bisquert, Physical Chemistry Chemical Physics **10**, 4478 (2008).
- <sup>17</sup> J. Gonzalez-Vazquez, J. A. Anta, and J. Bisquert, Physical Chemistry Chemical Physics **11**, 10359 (2009).
- <sup>18</sup> J. Gonzalez-Vazquez, J. A. Anta, and J. Bisquert, The Journal of Physical Chemistry C **114**, 8552 (2010).
- <sup>19</sup> J. Gonzalez-Vazquez, V. Morales-Flórez, and J. A. Anta, The journal of physical chemistry letters **3**, 386 (2012).
- <sup>20</sup> J. P. Gonzalez-Vazquez, G. Bigeriego, and J. A. Anta, Molecular Simulation **38**, 1242 (2012).
- <sup>21</sup> M. Ansari-Rad, Y. Abdi, and E. Arzi, Journal of Applied Physics **112**, 074319 (2012).
- <sup>22</sup> N. Abdi, Y. Abdi, E. N. Oskooee, and M. Sajedi, Journal of nanoparticle research **16**, 1 (2014).
- <sup>23</sup> M. Javadi and Y. Abdi, Journal of Applied Physics **118**, 064304 (2015).
- <sup>24</sup> N. Abdi, Y. Abdi, Z. Alemipour, and E. NedaaeeOskooee, Solar Energy **135**, 506 (2016).
- <sup>25</sup> J. van de Lagemaat, N. Kopidakis, N. R. Neale, and A. J. Frank, Physical Review B **71**, 035304 (2005).
- <sup>26</sup> R. Sibatov and E. Morozova, Journal of Experimental and Theoretical Physics **120**, 860 (2015).

<sup>27</sup> M. Mesta, C. Schaefer, J. De Groot, J. Cottaar, R. Co-echoorn, and P. Bobbert, *Physical Review B* **88**, 174204 (2013).

<sup>28</sup> J. van de Lagemaat, K. Zhu, K. D. Benkstein, and A. J. Frank, *Inorganica Chimica Acta* **361**, 620 (2008).

<sup>29</sup> R. Sibatov and V. Uchaikin, *Journal of Computational Physics* **293**, 409 (2015).

<sup>30</sup> M. Javadi, Y. Abdi, and E. Arzi, *Solar Energy* **133**, 549 (2016).

<sup>31</sup> J. A. Anta and V. Morales-Flórez, *The Journal of Physical Chemistry C* **112**, 10287 (2008).

<sup>32</sup> I. Fishchuk, A. Kadašchuk, S. Hoffmann, S. Athanasiopoulos, J. Genoe, H. Bässler, and A. Köhler, *Physical Review B* **88**, 125202 (2013).